

Cerium-Hydride Secondary Building Units in a Porous Metal–Organic Framework for Catalytic Hydroboration and Hydrophosphination

Pengfei Ji,[†] Takahiro Sawano,[†] Zekai Lin, Ania Urban, Dean Boures, and Wenbin Lin*

Department of Chemistry, University of Chicago, 929 East 57th Street, Chicago, Illinois 60637, United States

S Supporting Information

ABSTRACT: We report the stepwise, quantitative transformation of $\text{Ce}^{\text{IV}}(\mu_3\text{-O})_4(\mu_3\text{-OH})_4(\text{OH})_6(\text{OH}_2)_6$ nodes in a new Ce-BTC (BTC = trimesic acid) metal–organic framework (MOF) into the first $\text{Ce}^{\text{III}}(\mu_3\text{-O})_4(\mu_3\text{-OLi})_4(\text{H})_6(\text{THF})_6\text{Li}_6$ metal-hydride nodes that effectively catalyze hydroboration and hydrophosphination reactions. CeH-BTC displays low steric hindrance and electron density compared to homogeneous organolanthanide catalysts, which likely accounts for the unique 1,4-regioselectivity for the hydroboration of pyridine derivatives. MOF nodes can thus be directly transformed into novel single-site solid catalysts without homogeneous counterparts for sustainable chemical synthesis.

Lanthanide (Ln) catalysts are used for a wide range of reactions, including polymerization,¹ hydroamination,² hydrogenation,^{1c,2c} hydroboration,^{2c,3} Diels–Alder reactions,^{1c,4} and Aldol reactions.^{1c,5} They are more naturally abundant, less toxic, and more tolerant of certain functional groups, such as phosphines, than precious metal catalysts.^{1c} While most lanthanide catalysts are based on La, Sm, and Lu, little effort has been devoted to designing effective catalysts based on Ce, which is not only cheaper and more abundant but also broadly applied in stoichiometric organic transformations.⁶ Furthermore, Ln catalysts are often supported on sterically hindered ligands such as $\eta^5\text{-C}_5\text{Me}_5$ (Cp^*) to prevent oligomerization and disproportionation, which restricts the ability to fine-tune their electronic and steric properties. Although some elaborately designed ligands, such as $\text{Me}_2\text{Si}(\text{Cp}^*)_2$, can increase the open space around Ln centers, they typically require lengthy and laborious syntheses.⁷ We thus aimed to develop new synthetic strategies to produce Ln catalysts with low steric hindrance and different electronic properties.

Metal–organic frameworks (MOFs) provide a unique approach to developing highly active, reusable, single-site solid catalysts based on molecular species⁸ via direct solvothermal synthesis⁹ or postsynthetic functionalization.¹⁰ All components of MOFs, including their inorganic nodes,¹¹ organic linkers,¹² and void spaces,¹³ have been used to install catalytic species. In particular, straightforward functionalization of MOF nodes provides an intriguing opportunity to design single-site solid catalysts that do not have homogeneous counterparts. To date, however, the applications of MOF nodes have mostly focused on Lewis or Brønsted acid catalysts¹⁴ or as ligand sites that support other catalytic species.^{11,15}

Herein we report the direct transformation of $\text{Ce}^{\text{IV}}(\mu_3\text{-O})_4(\mu_3\text{-OH})_4(\text{OH})_6(\text{OH}_2)_6$ nodes in a new Ce-BTC (BTC = trimesic acid) MOF into previously unknown $\text{Ce}^{\text{III}}(\mu_3\text{-O})_4(\mu_3\text{-OLi})_4(\text{H})_6(\text{THF})_6\text{Li}_6$ metal-hydride nodes within the MOF¹⁶ and their use in the catalytic hydroboration of pyridines and alkenes, as well as the hydrophosphination of alkenes. The CeH-BTC catalyst exhibits high activity and unique regioselectivity, likely a result of its low steric hindrance and electron density compared to existing homogeneous lanthanide catalysts.

Ce-BTC was synthesized in 54% yield by treating $(\text{NH}_4)_2\text{Ce}(\text{NO}_3)_6$ with H_3BTC in a mixture of DMF and H_2O at 100 °C (Figure 1a). The structure of Ce-BTC was modeled using the crystal structure of Zr-BTC (MOF-808) by elongating the Ce– $\mu_3\text{-O}$ distance to 2.25 Å (from a Zr– $\mu_3\text{-O}$ distance of 2.16 Å).¹⁷ Similarities between powder X-ray diffraction (PXRD) patterns of as-synthesized Ce-BTC and the simulated pattern confirmed the *spn* topology (Figure 1b). We believe that the Ce centers possess square antiprismatic geometry, with a composition of $[(\mu_3\text{-O})_2(\mu_3\text{-OH})_2(\mu_2\text{-CO}_2^-)_2]\text{Ce}(\text{OH})(\text{OH}_2)$ (see below), similar to the Zr coordination in MOF-808. As Ce^{4+} has a larger ionic radius than Zr^{4+} [$r(\text{Ce}^{4+}) = 0.97$ Å and $r(\text{Zr}^{4+}) = 0.84$ Å], the Ce_6 node in Ce-BTC is larger than the Zr_6 node in MOF-808, with a Ce–Ce distance of 3.74 Å vs the Zr–Zr distance of 3.57 Å.

N_2 sorption isotherms of Ce-BTC at 77 K gave a Brunauer–Emmett–Teller (BET) surface area of 1008 m^2/g and a largest pore size of 22 Å, which corresponds well to the size of the hexagonal pore in the simulated structure of Ce-BTC (Figure 1a). The Ce oxidation state of Ce-BTC was studied by X-ray adsorption near-edge spectroscopy (XANES) and compared to $(\text{NH}_4)_2\text{Ce}^{\text{IV}}(\text{NO}_3)_6$ and $\text{Ce}^{\text{III}}\text{Cl}_3$ standards. Ce-BTC shows two XANES peaks at 5730 and 5738 eV (Figure 2b), which are identical to the Ce^{IV} standard, indicating the +4 oxidation state in Ce-BTC. We attributed the stability of Ce^{IV} toward potential reductants, including DMF and water, to carboxylate coordination.^{6b} ^1H NMR of digested Ce-BTC in $\text{D}_3\text{PO}_4/\text{DMSO}-d_6$ showed only the peaks of H_3BTC and adsorbed solvents, consistent with the coordination of H_2O and OH^- to Ce^{IV} (Figure S7, Supporting Information (SI)). Extended X-ray adsorption fine-structure (EXAFS) fitting of the Ce region supported the proposed structural model, with a Ce–OH/Ce– OH_2 average distance of 2.43 Å, close to typical $\text{Ce}^{\text{(IV)}}\text{–O}$ distances (Figure S3, SI).¹⁸

The Ce coordination environment of $[(\mu_3\text{-O})_2(\mu_3\text{-OH})_2(\mu_2\text{-CO}_2^-)_2]\text{Ce}(\text{OH})(\text{OH}_2)$ in Ce-BTC is analogous to those of

Received: September 24, 2016

Published: October 28, 2016



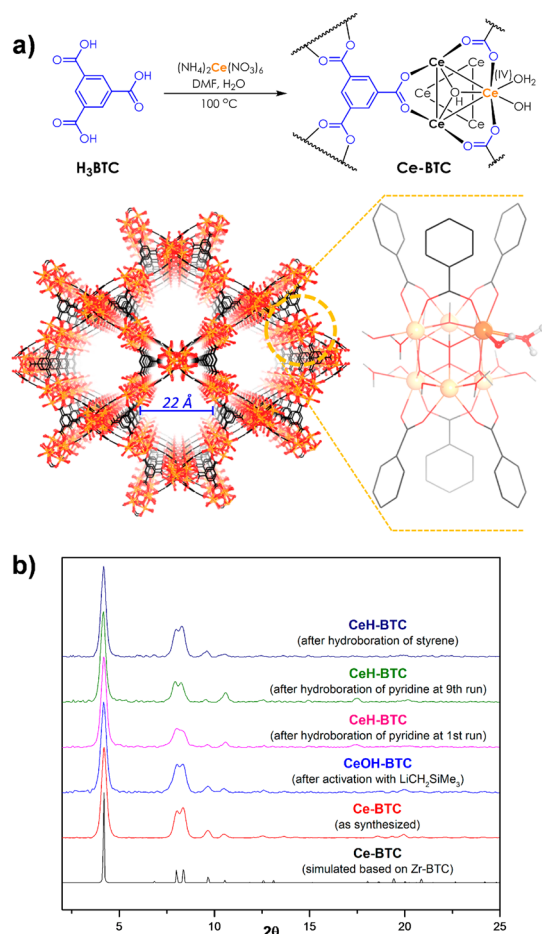


Figure 1. (a) Synthesis and a structural model of the Ce-BTC MOF. (b) Similarities between the PXRD patterns of Ce-BTC (red), CeOH-BTC (blue), CeH-BTC recovered from hydroboration of pyridine (pink and green) and hydroboration of styrene (navy blue) indicate the retention of crystallinity after activation and catalysis.

$\text{Ce}_2\text{Ln}(\text{X})(\text{L})$ (X = anionic ligand and L = neutral ligand) which have been used in many catalytic reactions. A structural model of Ce-BTC indicates that Ce–OH and Ce–OH₂ moieties point toward the large channel, affording low steric hindrance around the Ce centers. We thus sought to activate the Ce(OH)(OH₂) sites to prepare active Ce catalysts that are readily accessible to organic substrates via the large open channels of Ce-BTC.

Ce-BTC was activated by sequential deprotonation with $\text{LiCH}_2\text{SiMe}_3$ and reduction with pinacolborane (HBpin) to generate the first MOF-supported Ce-hydride catalyst for several important organic transformations (Figure 2a). The lithiated MOF, denoted CeOH-BTC, was obtained by treating Ce-BTC with 10 equiv of $\text{LiCH}_2\text{SiMe}_3$ (w.r.t. Ce), which deprotonated $(\mu_3\text{-OH})\text{Ce}(\text{OH})(\text{OH}_2)$ to form $[(\mu_3\text{-OLi})\text{Ce}(\text{OH})_2]\text{Li}$ and SiMe_4 . After removing CeOH-BTC, 1.74 ± 0.15 equiv of SiMe_4 (w.r.t. Ce) was detected in the supernatant by ^1H NMR, which corresponded well to the calculated result of 1.67 (Figure S9, SI). Inductively coupled plasma-mass spectrometry (ICP-MS) analysis of CeOH-BTC gave a Li-to-Ce ratio of 1.69 ± 0.05 , also matching our calculated result of 1.67.

CeOH-BTC was reduced to form CeH-BTC by treatment with HBpin at 60 °C in THF for 6 h (Figure 2a). GC analysis of the head space gas indicated the production of 0.5 equiv of H₂ (w.r.t. Ce). After removal of CeH-BTC, 2.02 ± 0.14 equiv of HOBpin (w.r.t. Ce) was detected in the supernatant by ^1H NMR, which

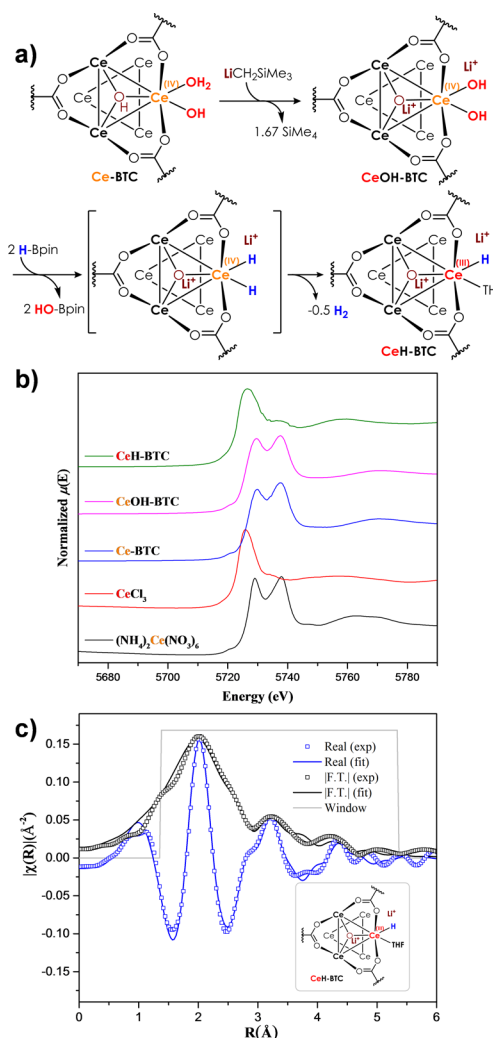


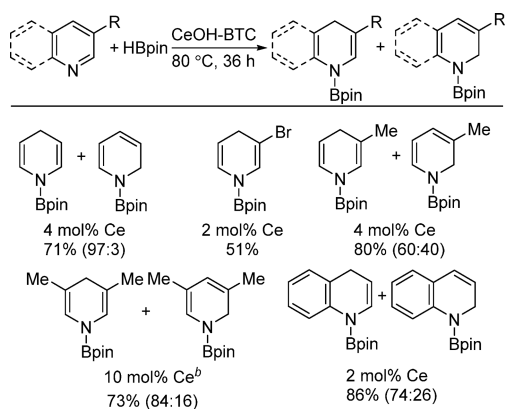
Figure 2. (a) Activation of Ce-BTC to form CeH-BTC. (b) XANES analysis of Ce-BTC (blue), CeOH-BTC (pink), and CeH-BTC (green) shows the reduction of Ce^{IV} in CeOH-BTC to Ce^{III} in CeH-BTC. (c) XAFS fitting on CeH-BTC confirms the proposed structure for the catalytic species. The R factor is 0.0146.

corresponded to our calculated result (2 equiv) (Figure S11, SI). We confirmed the identity of HOBpin using ^{11}B NMR ($\delta = 22.7$ ppm, 128 MHz) (Figure S10, SI). Based on the formation of 0.5 equiv of H₂ and 2 equiv of HOBpin, we propose that the reduction occurred via an H/OH exchange between HBpin and Ce(OH)₂ to form Ce^{IV}(H)₂ and HOBpin, followed by bimetallic reductive elimination of H₂ from neighboring Ce^{IV}(H)₂ species to form Ce^{III}H(THF). XANES of CeH-BTC showed a single Ce peak at 5726 eV, identical to the absorption feature of CeCl₃ (Figure 2b). Treatment of CeH-BTC with hydrochloric acid generated 0.98 ± 0.11 equiv of H₂, while no H₂ was observed when Ce-BTC or CeOH-BTC was treated with hydrochloric acid (Figure S13, SI). The PXRD pattern of CeH-BTC is identical to that of Ce-BTC, indicating that the MOF framework remains intact after lithiation and reduction (Figure 1b). EXAFS fitting at the Ce edge corresponded to our proposed CeH(THF) coordination model, with an R -factor of 0.015 (Figure 2c). EXAFS fitting afforded a Ce^{III}–($\mu_3\text{-O}$) distance of 2.44 Å in CeH-BTC, slightly longer than the Ce^{IV}–($\mu_3\text{-O}$) distance of 2.25 Å in CeOH-BTC, which is consistent with the increase of Ce ionic radius upon reduction.^{6b} We expect that the $[(\mu_3\text{-O})_2(\mu_3\text{-OH})_2(\mu_2\text{-CO}_2^-)_2]\text{Ce}$ moiety is

less electron-rich than other organolanthanide fragments, such as Cp^*_2Ln , potentially endowing the CeH-BTC catalyst with unique activity and selectivity.

CeH-BTC demonstrates high activity for several catalytic reactions and distinct selectivities from other lanthanide catalysts. Because 1,4-dihydropyridine is an important building block of natural products,¹⁹ biologically active intermediates,²⁰ and reducing reagents,²¹ we tested the activity of CeH-BTC for the hydroboration of pyridines with HBpin (Chart 1). Although

Chart 1. CeH-BTC Catalyzed 1,4-Selective Hydroboration of Pyridine Derivatives^a



^aNMR yield based on mesitylene as an internal standard. ^b110 °C.

hydroboration of pyridines provides a convenient synthetic route to 1,4-dihydropyridines, only one organoborane catalyst and one ruthenium catalyst were reported to effect 1,4-selective hydroboration reactions.^{22,23} Reaction of pyridine with HBpin with 4 mol % CeH-BTC catalyst loading at 80 °C for 36 h selectively gave the 1,4-addition product in 71% yield.²⁴ The hydroboration of pyridines by CeH-BTC has a broad substrate scope. With a 2 or 4 mol % catalyst loading, CeH-BTC was able to convert 3-bromopyridine and 3-methylpyridine to their corresponding 1,4-addition products along with small amounts of 1,2-addition products. We could also hydroborate 3,5-disubstituted pyridines, such as 3,5-dimethylpyridine, with 10 mol % CeH-BTC. CeH-BTC also exhibited good hydroboration activity for quinoline.

CeH-BTC is also active in the hydroboration of alkenes, a useful catalytic reaction in organic synthesis.²⁵ Reacting styrene and 1.5 equiv of HBpin with 0.1 mol % CeH-BTC catalyst loading at 80 °C for 18 h selectively gave the anti-Markovnikov-type addition product in 40% yield (entry 1, Table 1).²⁴ Increasing the catalyst loading to 0.5 mol % afforded the addition product in 79% yield (entry 2, Table 1). Hydroboration proceeded for several kinds of alkenes that we tested. Hydroboration of 4-fluorostyrene gave the corresponding addition product in high yield (entry 3, Table 1). Aliphatic alkenes, such as allylbenzene and 1-octene, were also used in hydroboration (entries 4 and 5, Table 1). α -Methylstyrene, a disubstituted alkene, was also a good substrate (entry 6, Table 1).

Hydrophosphination of alkenes is a powerful, direct, and atom-economical method for obtaining organophosphines,²⁶ an important class of compounds for chemical, agrochemical, pharmaceutical industries.²⁷ Moreover, organophosphines are among the most important ligands in homogeneous catalysis. While several examples of hydrophosphination of alkenes have been reported, the scope of substrates is limited, and examples of hydrophosphination of unactivated aliphatic olefins are rare.²⁸

Table 1. CeH-BTC Catalyzed Hydroboration of Alkenes

Entry	Substrate	Catalyst Loading (mol% Ce)	Yield (%) ^a
1		0.1	40
2		0.5	79
3		1	99
4 ^b		1	90
5 ^b		1	97
6 ^{b,c}		1	56

^aNMR yield using CH_3NO_2 as an internal standard. ^b36 h. ^c100 °C.

CeH-BTC catalyzed hydrophosphination of various unactivated alkenes. At 4 mol % Ce-loading, hydrophosphination of 1-octene for 18 h yielded 74% of *n*-octyldiphenylphosphine (entry 1, Table 2). Prolonging the reaction to 5 d afforded the addition product in

Table 2. CeH-BTC Catalyzed Hydrophosphination of Alkenes

Entry	Substrate	Product	Cat. Loading (mol% Ce)	Yield (%) ^a
1 ^b			4	74
2			4	99
3			4	75
4			4	80
5			12	50
6 ^c			12	41

^a¹H NMR yield was determined by CH_3NO_2 as an internal standard. ^b18 h. ^c100 °C.

99% yield (entry 2, Table 2). Hydrophosphination also proceeded for 1-decene and 6-chlorohexene (entries 3 and 4, Table 2). CeH-BTC displayed good activity for 2-methyl-1-pentene, an α -substituted alkene (entry 5, Table 2). The hydrophosphination of *cis*- β -methylstyrene with HPPH₂ gave 41% of the addition product (entry 6, Table 2).

We conducted several experiments to demonstrate the heterogeneity of CeH-BTC. First, we showed that the PXRD of CeH-BTC recovered from hydroboration of pyridines and alkenes remained the same as that of freshly prepared CeH-BTC. Second, we used ICP-MS to show that the amounts of Ce leaching into the supernatant during the hydroboration of pyridine and styrene and the hydrophosphination of 1-octene were less than 0.6%, 0.75%, and 0.03%, respectively. Finally, CeH-BTC could be recovered and reused 1 to 7 times without any loss of activity in each of the above reactions (Schemes S1–S3, SI).

In summary, we synthesized the new Ce-BTC MOF with a $\text{Ce}^{\text{IV}}(\mu_3\text{-O})_4(\mu_3\text{-OH})_4(\text{OH})_6(\text{OH}_2)_6$ SBU and transformed the SBU into a $\text{Ce}^{\text{III}}(\mu_3\text{-O})_4(\mu_3\text{-OLi})_4(\text{H})_6(\text{THF})_6\text{Li}_6$ node, which acts as an active catalyst for the selective hydroboration of pyridine and alkenes and hydrophosphination of alkenes. The CeH-BTC catalyst displayed lower steric hindrance and electron density than other lanthanide catalysts, which likely accounts for the unique 1,4-regioselectivity for the hydroboration of pyridine. MOF nodes thus have great potential for transformation into single-site solid catalysts without homogeneous counterparts for sustainable chemical synthesis.

■ ASSOCIATED CONTENT

Supporting Information

The Supporting Information is available free of charge on the ACS Publications website at DOI: 10.1021/jacs.6b10055.

General experimental section; synthesis and characterization of Ce-BTC, CeOH-BTC, and CeH-BTC; MOF catalyzed hydroboration and hydrophosphination (PDF)

■ AUTHOR INFORMATION

Corresponding Author

*wenbinlin@uchicago.edu

Author Contributions

[†]P.J. and T.S. contributed equally.

Notes

The authors declare no competing financial interest.

■ ACKNOWLEDGMENTS

This work was supported by the NSF (DMR-1308229). We thank G. Lan and M. Piechowicz for experimental help. XAS analysis was performed at Beamline 10BM-B, supported by the Materials Research Collaborative Access Team (MRCAT) and Beamline 9-BM, Advanced Photon Source (APS), Argonne National Laboratory (ANL). Use of the Advanced Photon Source, an Office of Science User Facility operated for the U.S. DOE Office of Science by ANL, was supported by the U.S. DOE under Contract No. DE-AC02-06CH11357.

■ REFERENCES

- (1) (a) Gromada, J.; Carpentier, J.-F.; Mortreux, A. *Coord. Chem. Rev.* **2004**, *248*, 397. (b) Hou, Z.; Wakatsuki, Y. *Coord. Chem. Rev.* **2002**, *231*, 1. (c) Kobayashi, S. *Lanthanides: chemistry and use in organic synthesis*; Springer: New York, 1999.
- (2) (a) Müller, T. E.; Hultsch, K. C.; Yus, M.; Foubelo, F.; Tada, M. *Chem. Rev.* **2008**, *108*, 3795. (b) Hong, S.; Marks, T. J. *Acc. Chem. Res.* **2004**, *37*, 673. (c) Molander, G. A.; Romero, J. A. C. *Chem. Rev.* **2002**, *102*, 2161.
- (3) Beletskaya, I.; Pelter, A. *Tetrahedron* **1997**, *53*, 4957.
- (4) Kobayashi, S.; Sugiura, M.; Kitagawa, H.; Lam, W. W.-L. *Chem. Rev.* **2002**, *102*, 2227.
- (5) Shibasaki, M.; Yoshikawa, N. *Chem. Rev.* **2002**, *102*, 2187.
- (6) (a) Sridharan, V.; Menéndez, J. C. *Chem. Rev.* **2010**, *110*, 3805. (b) Piro, N. A.; Robinson, J. R.; Walsh, P. J.; Schelter, E. J. *Coord. Chem. Rev.* **2014**, *260*, 21. (c) Nair, V.; Deepthi, A. *Chem. Rev.* **2007**, *107*, 1862. (d) Nair, V.; Balagopal, L.; Rajan, R.; Mathew, J. *Acc. Chem. Res.* **2004**, *37*, 21. (e) Vivier, L.; Duprez, D. *ChemSusChem* **2010**, *3*, 654.
- (7) (a) Jeske, G.; Schock, L. E.; Swepston, P. N.; Schumann, H.; Marks, T. J. *J. Am. Chem. Soc.* **1985**, *107*, 8103. (b) Fendrick, C. M.; Mintz, E. A.; Schertz, L. D.; Marks, T. J. *Organometallics* **1984**, *3*, 819.
- (8) Llabres i Xamena, F.; Gascon, J. *Metal Organic Frameworks as Heterogeneous Catalysts*; The Royal Society of Chemistry: Cambridge, 2013.
- (9) Zhao, Y.; Li, K.; Li, J. Z. *Naturforsch.* **2010**, *65b*, 976–998.
- (10) (a) Wang, Z.; Cohen, S. M. *Chem. Soc. Rev.* **2009**, *38*, 1315. (b) Tanabe, K. K.; Cohen, S. M. *Chem. Soc. Rev.* **2011**, *40*, 498.
- (11) (a) Manna, K.; Ji, P.; Greene, F. X.; Lin, W. *J. Am. Chem. Soc.* **2016**, *138*, 7488. (b) Klet, R. C.; Tussupbayev, S.; Borycz, J.; Gallagher, J. R.; Stalzer, M. M.; Miller, J. T.; Gagliardi, L.; Hupp, J. T.; Marks, T. J.; Cramer, C. J.; Delferro, M.; Farha, O. K. *J. Am. Chem. Soc.* **2015**, *137*, 15680. (c) Comito, R. J.; Fritzsche, K. J.; Sundell, B. J.; Schmidt-Rohr, K.; Dinca, M. *J. Am. Chem. Soc.* **2016**, *138*, 10232.
- (12) (a) Zhang, T.; Manna, K.; Lin, W. *J. Am. Chem. Soc.* **2016**, *138*, 3241. (b) Thacker, N. C.; Lin, Z.; Zhang, T.; Gilhula, J. C.; Abney, C. W.; Lin, W. *J. Am. Chem. Soc.* **2016**, *138*, 3501. (c) Falkowski, J. M.; Sawano, T.; Zhang, T.; Tsun, G.; Chen, Y.; Lockard, J. V.; Lin, W. *J. Am. Chem. Soc.* **2014**, *136*, 5213. (d) Manna, K.; Zhang, T.; Carboni, M.; Abney, C. W.; Lin, W. *J. Am. Chem. Soc.* **2014**, *136*, 13182.
- (13) (a) Genna, D. T.; Wong-Foy, A. G.; Matzger, A. J.; Sanford, M. S. *J. Am. Chem. Soc.* **2013**, *135*, 10586. (b) Choi, K. M.; Na, K.; Somorjai, G. A.; Yaghi, O. M. *J. Am. Chem. Soc.* **2015**, *137*, 7810. (c) Wang, C.; deKrafft, K. E.; Lin, W. B. *J. Am. Chem. Soc.* **2012**, *134*, 7211.
- (14) Jiang, J.; Yaghi, O. M. *Chem. Rev.* **2015**, *115*, 6966–6997.
- (15) (a) Phan, A.; Czaja, A. U.; Gándara, F.; Knobler, C. B.; Yaghi, O. M. *Inorg. Chem.* **2011**, *50*, 7388. (b) Xiao, D. J.; Bloch, E. D.; Mason, J. A.; Queen, W. L.; Hudson, M. R.; Planas, N.; Borycz, J.; Dzubak, A. L.; Verma, P.; Lee, K.; Bonino, F.; Crocellá, V.; Yano, J.; Bordiga, S.; Truhlar, D. G.; Gagliardi, L.; Brown, C. M.; Long, J. R. *Nat. Chem.* **2014**, *6*, 590. (c) Metzger, E. D.; Brozek, C. K.; Comito, R. J.; Dincă, M. *ACS Cent. Sci.* **2016**, *2*, 148.
- (16) Lammert, M.; Wharmby, M. T.; Smolders, S.; Bueken, B.; Lieb, A.; Lomachenko, K. A.; De Vos, D.; Stock, N. *Chem. Commun.* **2015**, *51*, 12578.
- (17) Furukawa, H.; Gándara, F.; Zhang, Y.-B.; Jiang, J.; Queen, W. L.; Hudson, M. R.; Yaghi, O. M. *J. Am. Chem. Soc.* **2014**, *136*, 4369.
- (18) Behrsing, T.; Bond, A. M.; Deacon, G. B.; Forsyth, C. M.; Forsyth, M.; Kamble, K. J.; Skelton, B. W.; White, A. H. *Inorg. Chim. Acta* **2003**, *352*, 229.
- (19) (a) Bull, J. A.; Mousseau, J. J.; Pelletier, G.; Charette, A. B. *Chem. Rev.* **2012**, *112*, 2642. (b) Lavilla, R. J. *Chem. Soc., Perkin Trans.* **2002**, *1*, 1141. (c) Stout, D. M.; Meyers, A. *Chem. Rev.* **1982**, *82*, 223.
- (20) Edraki, N.; Mehdipour, A. R.; Khoshneviszadeh, M.; Miri, R. *Drug Discovery Today* **2009**, *14*, 1058.
- (21) (a) Zheng, C.; You, S.-L. *Chem. Soc. Rev.* **2012**, *41*, 2498. (b) Rueping, M.; Dufour, J.; Schoepke, F. R. *Green Chem.* **2011**, *13*, 1084. (c) Ouellet, S. G.; Walji, A. M.; Macmillan, D. W. *Acc. Chem. Res.* **2007**, *40*, 1327.
- (22) (a) Fan, X.; Zheng, J.; Li, Z. H.; Wang, H. *J. Am. Chem. Soc.* **2015**, *137*, 4916. (b) Kaithal, A.; Chatterjee, B.; Gunanathan, C. *Org. Lett.* **2016**, *18*, 3402.
- (23) (a) Intemann, J.; Lutz, M.; Harder, S. *Organometallics* **2014**, *33*, 5722. (b) Dudnik, A. S.; Weidner, V. L.; Motta, A.; Delferro, M.; Marks, T. J. *Nat. Chem.* **2014**, *6*, 1100. (c) Oshima, K.; Ohmura, T.; Sugimoto, M. *J. Am. Chem. Soc.* **2012**, *134*, 3699. (d) Arrowsmith, M.; Hill, M. S.; Hadlington, T.; Kociok-Köhn, G.; Weetman, C. *Organometallics* **2011**, *30*, 5556.
- (24) The reaction did not proceed with Ce-BTC or without catalyst.
- (25) (a) Beletskaya, I.; Pelter, A. *Tetrahedron* **1997**, *53*, 4957. (b) Burgess, K.; Ohlmeyer, M. J. *Chem. Rev.* **1991**, *91*, 1179. (c) Zhang, L.; Peng, D.; Leng, X.; Huang, Z. *Angew. Chem., Int. Ed.* **2013**, *52*, 3676.
- (26) (a) Koshti, V.; Gaikwad, S.; Chikkali, S. H. *Coord. Chem. Rev.* **2014**, *265*, 52. (b) Delacroix, O.; Gaumont, A. *Curr. Org. Chem.* **2005**, *9*, 1851.
- (27) Quin, L. D. *A guide to organophosphorus chemistry*; John Wiley & Sons: New York, 2000.
- (28) (a) Ghebreab, M. B.; Bange, C. A.; Waterman, R. *J. Am. Chem. Soc.* **2014**, *136*, 9240. (b) Leyva-Pérez, A.; Vidal-Moya, J. A.; Cabrero-Antonino, J. R.; Al-Deyab, S. S.; Al-Resayes, S. I.; Corma, A. *J. Organomet. Chem.* **2011**, *696*, 362.